JOURNAL OF GEOPHYSICAL RESEARCH, VOL. 114, G02016, doi:10.1029/2008JG000850, 2009

Global pattern of temperature sensitivity of soil heterotrophic respiration (Q_{10}) and its implications for carbon-climate feedback

Tao Zhou,[1,2] Peijun Shi,[1] Dafeng Hui,[3] and Yiqi Luo[2]

Received 31 August 2008; revised 12 March 2009; accepted 7 April 2009; published 27 May 2009.

[1] Temperature sensitivity of soil respiration (Q_{10}) is an important parameter in modeling effects of global warming on ecosystem carbon release. Experimental studies of soil respiration have ubiquitously indicated that Q_{10} has high spatial heterogeneity. However, most biogeochemical models still use a globally constant Q_{10} in projecting future climate change, partly because no spatial pattern of Q_{10} values has been derived. In this study, we conducted an inverse analysis to retrieve a global pattern of spatially heterogeneous Q_{10} values by assimilating data of soil organic carbon into a process-based terrestrial carbon model (Carnegie-Ames-Stanford Approach model) at spatial resolution of 1° by 1°. The estimated Q_{10} values were, in turn, incorporated into soil respiration models to evaluate their impacts on global respiratory carbon release from soil (i.e., total soil respiration is equal to microbial and root respiration) and from microbial decomposition (i.e., heterotrophic respiration). Our results show that the optimized Q_{10} values are spatially heterogeneous and vary with environmental factors. In general, Q_{10} value tends to be high in the high-latitudinal regions. The mean Q_{10} values for different biomes range from 1.43 to 2.03, with the highest value in tundra and the lowest value in deserts. When spatially heterogeneous Q_{10} values were incorporated into global soil respiration models, simulated soil respiration has a feedback intensity of 3.21 Pg C $°C^{-1}$ to climate warming, which is approximately 40% higher than that with a globally invariant Q_{10} value. The modeled heterotrophic respiration has a feedback intensity of 2.26 Pg C $°C^{-1}$, about 25% higher than that derived from a globally invariant Q_{10} value. Overall, the feedback intensity of soil carbon release to climate warming depends not only on the magnitude of a global mean of Q_{10} values but also their spatial variability.

Citation: Zhou, T., P. Shi, D. Hui, and Y. Luo (2009), Global pattern of temperature sensitivity of soil heterotrophic respiration (Q_{10}) and its implications for carbon-climate feedback, *J. Geophys. Res.*, *114*, G02016, doi:10.1029/2008JG000850.

1. Introduction

[2] Soil respiration in terrestrial ecosystems plays a critical role in regulating global carbon cycling. One significant factor that not only influences the response of soil respiration to global change but also determines the direction and magnitude of terrestrial carbon cycle feedback to climate warming is temperature sensitivity of soil respiration [*Schimel et al.*, 1994; *Luo*, 2007]. Temperature sensitivity of soil respiration (often termed as Q_{10}) is a factor by which soil respiration is multiplied when temperature increases by 10°C [*Davidson et al.*, 2006], which is an important parameter to evaluate the feedback intensity between soil carbon efflux and global warming [*Cox et al.*, 2000; *Luo et al.*, 2001; *Friedlingstein et al.*, 2003; *Reichstein et al.*, 2003]. So far, most models generally consider the temperature sensitivity as globally invariant when simulate global soil respiration [*Friedlingstein et al.*, 2006]. If the spatially heterogeneity in Q_{10} is considered, the direction and magnitude of the terrestrial carbon cycle feedbacks to climate warming could be significantly changed [*Jones et al.*, 2003]. It is an urgent need to derive the global pattern of Q_{10} and quantify its feedbacks in the terrestrial ecosystem carbon cycling to climate warming [*Holland et al.*, 2000; *Luo*, 2007].

[3] There are two kinds of definitions on temperature sensitivity, i.e., ''intrinsic temperature sensitivity'' and ''apparent temperature sensitivity'' [*Davidson and Janssens*, 2006]. The intrinsic temperature sensitivity is the theoretic sensitivity determined by molecular structure, while the latter is the observed temperature sensitivity determined by both molecular structure and environmental constraints caused by heterogeneous soil properties [*Sollins et al.*, 1996; *Davidson and Janssens*, 2006]. As environmental constrains dampen or obscure the intrinsic temperature sensitivity of substrate decomposition, the apparent (or observed) temperature sensitivity is usually less than expected value [*Davidson and Janssens*, 2006]. Hereafter,

[1]State Key Laboratory of Earth Surface Processes and Resource Ecology, Beijing Normal University, Beijing, China.
[2]Department of Botany and Microbiology, University of Oklahoma, Norman, Oklahoma, USA.
[3]Department of Biological Sciences, Tennessee State University, Nashville, Tennessee, USA.

0148-0227/09/2008JG000850$09.00

the temperature sensitivity (Q_{10}) in this study is stated for apparent temperature sensitivity.

[4] Experimental studies of Q_{10} have long and extensively been conducted in many ecosystems [*Luo and Zhou*, 2006]. Experimental results demonstrated that Q_{10} values varied with temperature [*Lloyd and Taylor*, 1994; *Kirschbaum*, 1995; *Luo et al.*, 2001], quantity and quality of soil organic matter [*Taylor et al.*, 1989; *Liski et al.*, 1999; *Wan and Luo*, 2003], soil moisture [*Davidson et al.*, 1998; *Reichstein et al.*, 2002; *Hui and Luo*, 2004], and land cover type [*Raich and Tufekcioglu*, 2000]. The Q_{10} values derived from measured soil respiration and temperature usually decline with temperature because substrate availability decreases as temperature increases [see *Tedla et al.*, 2009]. As described by the Michaelis-Menten kinetics equation, the low substrate availability generally results in a low Q_{10} value [*Davidson et al.*, 2006]. Soil water content influences temperature sensitivity because diffusivity of soluble substrates is low at low water content and diffusivity of oxygen is low at high water content. Low diffusivity of either soluble substrates at low water content or oxygen at high water content limits soil microbial respiration [*Davidson et al.*, 2006]. All the environmental and biological factors such as soil temperature, moisture, and soil organic matter are spatially heterogeneous. Accordingly, estimated Q_{10} from measured soil respiration likely varies spatially at different geographic locations [*Xu and Qi*, 2001].

[5] In the past, Q_{10} values have been seldom estimated using process-based modeling but mostly by regression analysis of measured soil CO_2 efflux rates against temperature [e.g., *Raich and Potter*, 1995; *Fang et al.*, 2005]. As empirical models do not contain equations to represent the underlying physical, chemical, and biological processes as described in the above paragraph, the estimated Q_{10} values may not reflect true temperature sensitivity of soil respiration. High values of Q_{10} estimates, such as those significantly higher than 2.5, may be caused by confounding factors, e.g., substrate supply [*Davidson et al.*, 2006]. In addition, reliability of the estimated Q_{10} values also depends on the precision of instruments used in soil CO_2 efflux measurement. The static chamber, for example, may underestimate soil respiration [*Raich et al.*, 2002].

[6] Inverse modeling can be potentially a useful method to estimate temperature sensitivity of soil respiration [*Raupach et al.*, 2005]. This method assimilates data from observations and experiments with a process-based biogeochemical model for parameter estimation. For example, *Ise and Moorcroft* [2006] applied an inverse modeling method to integration of a CENTURY-based mechanistic decomposition model with observed soil organic carbon content to estimate the optimal Q_{10} of soil respiration. On the basis of the TECO-R model and remote sensing data, inverse modeling was also used by *Zhou and Luo* [2008] to estimate spatial distribution of carbon residence times for plant and soil.

[7] In this study, we used an inverse modeling approach, which assimilates a process-based model (CASA model) with the measured soil organic carbon (SOC) [*Global Soil Data Task*, 2000] using a constraint of the global mean Q_{10} value of soil respiration reported by *Raich et al.* [2002] to retrieve a global distribution of spatially heterogeneous Q_{10} values at a resolution of 1° by 1°. Our approach assumed that temperature sensitivity of the heterogeneous respiration (Q_{10}) can be constrained by the Q_{10} value of soil respiration. Since the autotrophic component of soil respiration may be more sensitive than its heterotrophic component to temperature change [*Boone et al.*, 1998], the constraint may slightly overestimate Q_{10} values of the heterotrophic respiration. On the basis of the estimated Q_{10} values, we analyzed the statistical dependencies of Q_{10} values on environmental factors at the global scale. Finally, we used an empirical soil respiration model and a process-based model to evaluate the impacts of the spatially heterogeneous Q_{10} values on respiratory carbon release from soil (i.e., total soil respiration is equal to microbial and root respiration) and microbial decomposition (i.e., heterotrophic respiration), respectively, in response to climate warming. As it is difficult to separate a Q_{10} value for heterotrophic respiration and autotrophic respiration in soil at global scale, we assume the Q_{10} value for heterotrophic respiration equals that for root respiration at the same spatial grid.

2. Materials and Methods

[8] Our inversion approach is based on an assumption that at equilibrium, the soil carbon input from ecosystem production and output from soil respiration is balanced. The soil carbon output by soil respiration is closely related to a Q_{10} value [*Xu and Qi*, 2001; *Fang et al.*, 2005]. The latter varies with climatic factors [*Reichstein et al.*, 2003; *Hui and Luo*, 2004], and chemical compounds of plant litter and soil texture [*Schimel et al.*, 1994]. Since Q_{10} significantly regulates soil carbon release and then soil organic carbon (SOC) at a steady state with the yearly soil heterogeneous respiration equals ecosystem net primary production (NPP), SOC at particular geographical locations contains information on Q_{10}. Therefore, using the measured SOC as constraints, the optimal Q_{10} can be estimated based on a rule that the deviation of the observed and modeled Q_{10}-related SOC is minimized.

[9] In this study, NPP and SOC were estimated using Carnegie-Ames-Stanford Approach (CASA model), which contains an ecosystem production submodel and a soil carbon submodel [*Potter et al.*, 1993; *Field et al.*, 1995]. The model used in this study has been improved and validated by *Randerson et al.* [1996], *Potter and Klooster* [1997], and *Friedlingstein et al.* [1999]. The CASA model calculates NPP as a function of normalized difference vegetation index (NDVI), photosynthetically active radiation, maximum possible light utilization efficiency, temperature and precipitation. The soil carbon submodel simulates carbon cycling using a set of compartmental difference equations based on a simplified version of the CENTURY model [*Parton et al.*, 1987, 1988]. Carbon fluxes are controlled using nondimensional scalars related to air temperature, soil moisture, litter substrate quality (N and lignin contents), and soil texture. Carbon in soil organic form is represented by two storage pools: the SLOW pool, which chiefly contains chemically protected C, and the OLD pool, which mainly contains physically protected C. Fluxes from litter and soil to microbial pools and from microbial pools back to soil pools occur in proportion to C assimilation rates:

$$CO_2(x,t)_i = C(x,t)_i \cdot k_i \cdot W_s(x,t) \cdot T_s(x,t) \cdot (1 - M_\varepsilon) \quad (1)$$

where x and t represent spatial grid and time (month) respectively; $CO_2(x, t)_i$ is production of CO_2 of pool i, which results from microbe-mediated decomposition of soil organic carbon; $C(x, t)_i$ is carbon content of pool i; M_ε is carbon assimilation efficiency of microbes; $W_s(x, t)$ is scalar for the effect of soil moisture content on decomposition; $T_s(x, t)$ is scalar for the effect of temperature on decomposition, which was treated uniformly as an exponential (Q_{10}) response:

$$T_s(x,t) = Q_{10}^{[(T(x,t)-35)/10]} \tag{2}$$

where Q_{10} is temperature sensitivity of soil microbial respiration and $T(x, t)$ is monthly average air temperature.

2.1. Inversion Algorithm

[10] At each 1° by 1° spatial grid x, we searched for the optimal value of Q_{10} in the domain $Q \in [Q_{min}, Q_{max}]$ such that

$$\left|S_{m,x}\left(Q_{10}^0(Q)\right) - S_{0,x}\right| \le \left|S_{m,x}\left(Q'_{10}\right) - S_{0,x}\right|, \forall Q'_{10} \in Q \tag{3}$$

where $S_{0,x}$ is the measured SOC at grid x, which obtained directly from the SOC database [*Global Soil Data Task*, 2000]. $S_{m,x}(Q_{10}^0(Q))$ is CASA modeled SOC with the optimal Q_{10} value (Q_{10}^0), which is related with the searching domain Q. $S_{m,x}(Q'_{10})$ is modeled SOC with an arbitrary Q_{10} value (Q'_{10}) that locates in the domain Q. After the optimal Q_{10} values for all grids are estimated, the modeled global mean SOC in the domain Q has the minimal deviation with the global mean observations:

$$J(Q) = \frac{\sum_x \left|S_{m,x}\left(Q_{10}^0(x)\right) - S_{0,x}\right| \times a(x)}{\sum_x a(x)} \tag{4}$$

where $a(x)$ is grid area of x, and J is the global mean deviation between modeled and observed SOC, which depends on the optimal Q_{10} value of each grid and therefore related with the searching domain Q.

[11] The reasonable low limit (Q_{min}) of domain Q is relatively easy to assign. In this study Q_{min} equals 1, which means that soil respiration do not change with temperature; it usually appears at soil type of entisol where SOC is absent. The reasonable upper limit (Q_{max}), however, is somewhat difficult to define as the estimated upper limits from soil respiration measurements can be very high (e.g., significantly above 2.5), which probably can be attributed to some confounding effects from substrate supply and other processes [*Davidson et al.*, 2006].

[12] For this reason, we did not prescribe a prior Q_{max} value. Rather, we constrained the Q_{max} value according to the following considerations. The global mean Q_{10} value ($\overline{Q}_{10}$) has been estimated from worldwide soil respiration measurements [*Raich and Potter*, 1995; *Raich et al.*, 2002]. Our globally averaged Q_{10} value should be matched with this value derived from the measurements of soil respiration:

$$Q_g(Q_{max}) = \frac{\sum_x \left[a(x) \times Q_{10}^0(x)\right]}{\sum_x a(x)} \tag{5}$$

$$\left|Q_g - \overline{Q}_{10}\right| < 0.01 \tag{6}$$

where Q_g is the global mean Q_{10} value that related with optimal Q_{10} values of grids and therefore, related with the upper limit of domain (Q_{max}). The value of $\overline{Q}_{10}$ used in this study equals 1.72 as reported by *Raich et al.* [2002] from soil respiration measurements in major ecosystems of the world.

2.2. Data

[13] The spatial data sets used in this study include (1) vegetation type, soil texture, multiyear monthly mean AVHRR-NDVI and solar radiation (provided by Climatology Interdisciplinary Data Collection and issued by Distributed Active Archive Center at Goddard Space Flight Center, http://daac.gsfc.nasa.gov); (2) multiyear monthly mean temperature and precipitation data sets (provided by C. J. Willmott and K. Matsuura, http://climate.geog.udel.edu/~climate); and (3) the maps of soil organic carbon and nitrogen (provided by IGBP-DIS [*Global Soil Data Task*, 2000]). All of those global data sets were resampled to the same geographic projection and at spatial resolution of 1° by 1° in ERDAS IMAGINE 8.5.

[14] The observations of soil respiration used for verification came from the literature and compiled by *Raich et al.* [2002] and have been used to verify the Raich's soil respiration model. All of those soil respiration measurements were made with dynamic chambers coupled to infrared gas analyzers (IRGA).

2.3. Verification

[15] To verify if the spatial pattern of estimated Q_{10} values from the inversion algorithm is reasonable, we estimated soil respiration at several representative sites and compared them to the field measurements. As the spatially heterogeneous Q_{10} values were estimated from assimilation of the spatial pattern of observed SOC into the CASA model and further constraints by the global mean Q_{10} over worldwide soil respiration measurements, it was expected that the estimated Q_{10} values could improve fitness of modeled soil respiration to the measured one in comparison to that with the invariant Q_{10} in different spatial grids. To do so, we applied a statistic of root-mean squared errors (RMSE) to evaluate its improvement of modeled soil respiration using the spatially heterogeneous Q_{10} values estimated from this inverse analysis relative to those using a globally invariant Q_{10} in different spatial grids.

2.4. Evaluations of Spatial Patterns of Q_{10} on Modeling of Soil Respiration

[16] To evaluate the potential influences of spatially heterogeneous Q_{10} values on soil respiration modeling, we used an empirical soil respiration model as in the work of

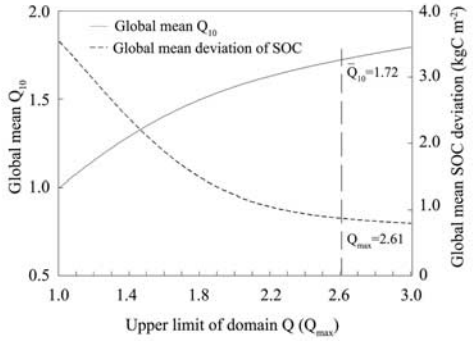

Figure 1. Relationship between optimal global mean Q_{10} value and upper limit of domain Q. As Q_{max} becomes larger, there are more chances to find a better Q_{10} by the inverse algorithm to minimize the deviation of the modeled SOC from the observed one. However, the rate of this improvement of the model-data match declines to be sufficiently small as Q_{max} becomes higher than 2.61, at which value the globally mean Q_{10} value ($\overline{Q}_{10}$) that derived from worldwide measurements of soil respirations is 1.72.

Raich et al. [2002] to simulate soil respiration (i.e., both soil heterotrophic respiration and root respiration), which is matched with field soil respiration measurements. In addition, we used a process-based model, the CASA soil carbon submodel, to simulate soil heterotrophic respiration, which accounts for simultaneous changes in soil C stocks and temperature sensitivity of soil respiration.

[17] The original Raich's model uses a global invariant Q_{10} value (Q_{10} = 1.72) and expresses as:

$$\text{Model A}: R_s = F \times e^{(b \times T_a)} \times [P/(K+P)] \tag{7}$$

where R_s refers to the mean monthly soil respiration in g C m^{-2} d^{-1}; b is a constant temperature sensitivity (b = $\mathrm{Ln}Q_{10}/10$ = 0.054); T_a refers to the mean monthly air temperature (°C), and P is the mean monthly precipitation (cm); F and K are constants (F = 1.250 and K = 4.259) derived from the observed soil respiration.

[18] The modified model uses the inverted global pattern of Q_{10} values and expresses as:

$$\text{Model B}: R_s' = F \times e^{(b_x \times T_a)} \times [P/(K+P)] \tag{8}$$

where b_x is our estimated temperature sensitivity at spatial grid x (b_x = $\mathrm{Ln}Q_{10}(x)/10$); R_s' refers to the mean monthly soil respiration with spatially heterogeneous Q_{10} values in g C m^{-2} d^{-1}.

[19] We selected Raich's model because it is developed upon the worldwide measurements of soil respiration. In addition, the global mean value of our inverted Q_{10} is the same with the Raich's global invariant Q_{10} value (i.e., Q_{10} = 1.72), so the deviation of total modeled soil respiration is completely induced by the spatial distribution of Q_{10} values.

[20] We also evaluated potential impacts of spatially heterogeneous Q_{10} on carbon cycle–climate change feedback via soil respiration under two scenarios. The first one is a 1°C increase of temperature evenly in each spatial grid. The second one is the actual interannual variations of temperature observed from 1982 to 1999 [*Legates and Willmott*, 1990a, 1990b]. In both scenarios, soil respiration was modeled simultaneously by empirical models A and B, while the soil heterotrophic respiration was modeled by CASA soil carbon submodel, in which the spatially heterogeneous and the globally invariant Q_{10} were both used.

3. Results

3.1. Global Pattern of Q_{10}

[21] At the global scale, the optimal mean Q_{10} value increases but the mean deviation between the modeled and observed SOC decreases with the upper limit of domain Q (i.e., Q_{max}) (Figure 1). As Q_{max} becomes larger, there are

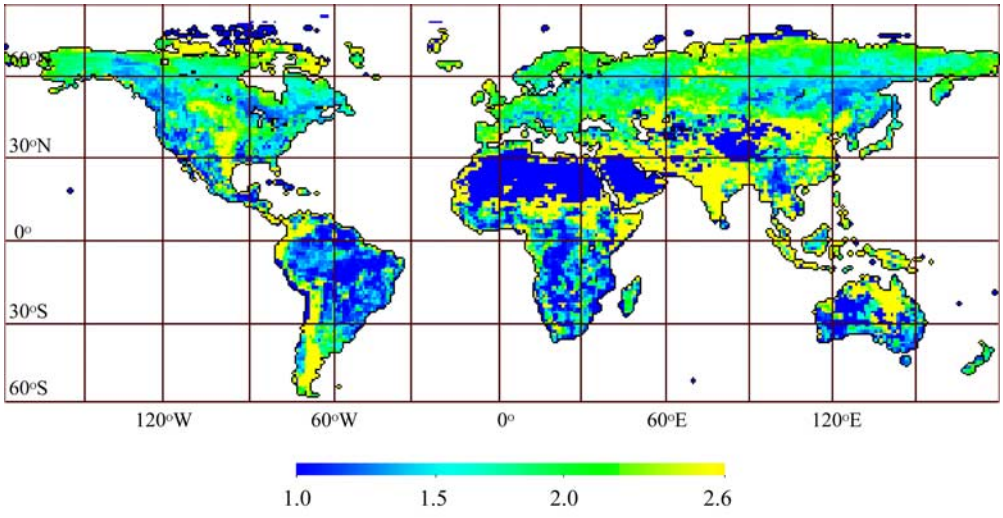

Figure 2. Spatial pattern of the optimal Q_{10} values. In general, tundra, C3 and C4 grasslands, shrublands, and croplands have higher Q_{10} values than deserts, bare grounds, broadleaf deciduous forests, and woodlands.

Table 1. Area-Weighted Mean Values of Q_{10}, Mean Annual Temperature, and Mean Annual Precipitation for Each Land Cover Type[a]

Land Cover Type[b]	Number of Grids	Area (km^2)	Q_{10}	MAT[c] (°C)	MAP[d] (mm a^{-1})
Broadleaf evergreen forest	1093	1.34E+07	1.50	25.0	2201
Broadleaf deciduous forest and woodland	318	3.28E+06	1.75	16.6	961
Mixed forest and woodland	763	6.55E+06	1.61	9.2	934
Coniferous forest and woodland	2000	1.29E+07	1.69	−2.1	547
High-latitude deciduous forest and woodland	952	5.75E+06	1.61	−5.7	442
Wooded C_4 grassland	1456	1.71E+07	1.59	23.1	1324
C_4 grassland	779	8.93E+06	2.02	23.8	580
Shrubs	1034	1.10E+07	1.82	17.6	266
Tundra	1507	7.00E+06	2.03	−10.4	335
Desert, bare ground	1598	1.68E+07	1.43	20.6	96
Cultivation	1368	1.33E+07	2.01	14.7	832
C_3 wooded grassland	440	4.46E+06	1.66	14.6	1145
C_3 grassland	1235	1.14E+07	1.96	7.3	423
All, global average[e]	14543	1.32E+08	1.72	13.7	789

[a]MAT, mean annual temperature; MAP, mean annual precipitation.
[b]The original land cover classification was produced by R. DeFries and J. Townshend (Department of Geography, University of Maryland at College Park), with revisions made by J. Collatz (Code 923, NASA Goddard Space Flight Center).
[c]Area-weighted annual mean temperature.
[d]Area-weighted annual total precipitation.
[e]Antarctica and ice are excluded.

more chances to find a better Q_{10} by the inverse algorithm to minimize the deviation of the modeled SOC from the observed one in any particular spatial grid. However, the rate of this improvement of the model-data match declines to be sufficiently small as Q_{max} becomes higher than 2.61, at which the globally mean Q_{10} value ($\overline{Q}_{10}$) is 1.72. The latter was derived from worldwide measurements of soil respirations. Thus, the globally mean Q_{10} value of 1.72 is an effective constraint in our inverse analysis to retrieve optimal Q_{10} values from observed SOC in individual spatial grids. It also suggests that the Q_{10} values derived from measured soil respiration are, on average, consistent with those estimated from our inverse analysis that assimilated observed SOC into a process-based carbon cycle model.

[22] The derived spatial pattern of the optimal Q_{10} values at global scale shows a great spatial heterogeneity (Figure 2). The optimal Q_{10} values for each biome range from the lowest of 1.43 for desert and bare ground to the highest of 2.03 for tundra (Table 1). In general, tundra, C3 and C4 grasslands, shrublands, and croplands have higher Q_{10} values than deserts, bare grounds, broadleaf deciduous forests, and woodlands. The optimal Q_{10} values are relatively higher in the higher-latitude regions as reflected by a positive correlation between latitudes (°) and the latitudinal mean Q_{10} values ($r = 0.51$).

3.2. Comparison of Modeled With Observed Soil Respiration

[23] Incorporation of site-specific Q_{10} values into the model B (equation (8)) consistently improved simulated soil respiration in comparison with those with the invariant Q_{10} in model A (equation (7)) at all sites (Figure 3). The root-mean squared errors (RMSE) between the modeled and observed soil respiration decrease by 3.1 to 30.0% for different sites with the site-specific Q_{10} values than the globally invariant Q_{10} values. For instance, RMSE of a deciduous forest in USA (43.1°N, 70.0°W) is 0.61 when using our estimated Q_{10} of 1.80, while the corresponding RMSE is 0.73 when using a constant Q_{10} of 1.72. Thus, the RMSE decreased by 16.4%.

3.3. Statistical Dependency of Q_{10} on Environmental Factors

[24] Correlation analysis indicates that the Q_{10} values estimated by our inverse method are statistically related with environmental factors such as soil organic carbon content and mean annual precipitation (MAP). Q_{10} values are positively correlated with soil organic carbon and soil nitrogen contents, with the correlation coefficients of 0.30 and 0.31, respectively (Table 2). The correlation between Q_{10} and MAP is positive for the broadleaf evergreen forests, broadleaf deciduous forests, grassland, cultivation, and desert and bare ground but negative for needleleaf forests and high-latitude deciduous forest.

3.4. Impacts of Q_{10} on Global Soil Respiration Modeling

[25] Under the first scenario with an even increase in temperature by 1°C for each spatial grid, simulated soil respiration by the empirical model A with globally invariant Q_{10} is considerably different from that by the model B with spatially heterogeneous Q_{10} (Figures 4a and 4b). The relative discrepancy between the two models is larger than ±5% (Figure 4b). The absolute discrepancy of the simulated soil respiration between the two models is largest in the latitude band of 0°–30°N and quite minor in the latitude bands of 60–90°N and 30°–60°S. At the global scale, the increment of modeled soil respiration with the spatially heterogeneous Q_{10} values is 7.02 Pg C a^{-1} in response to climate warming by 1°C, which is much higher than 4.16 Pg C a^{-1} estimated with an globally invariant Q_{10} value. Thus, the feedback intensity between soil respiration and climate warming would be underestimated by 40.7% if the spatially heterogeneous Q_{10} values were not considered.

[26] Under the first scenario, soil heterotrophic respiration simulated by the CASA soil carbon submodel displays a similar spatial pattern of relative discrepancy between the spatially heterogeneous and invariant Q_{10} (Figure 4d), but the absolute discrepancy between the two types of Q_{10} in simulated heterotrophic respiration by the CASA model is apparently less than total respiration by the empirical models (Figure 4a versus Figure 4c).

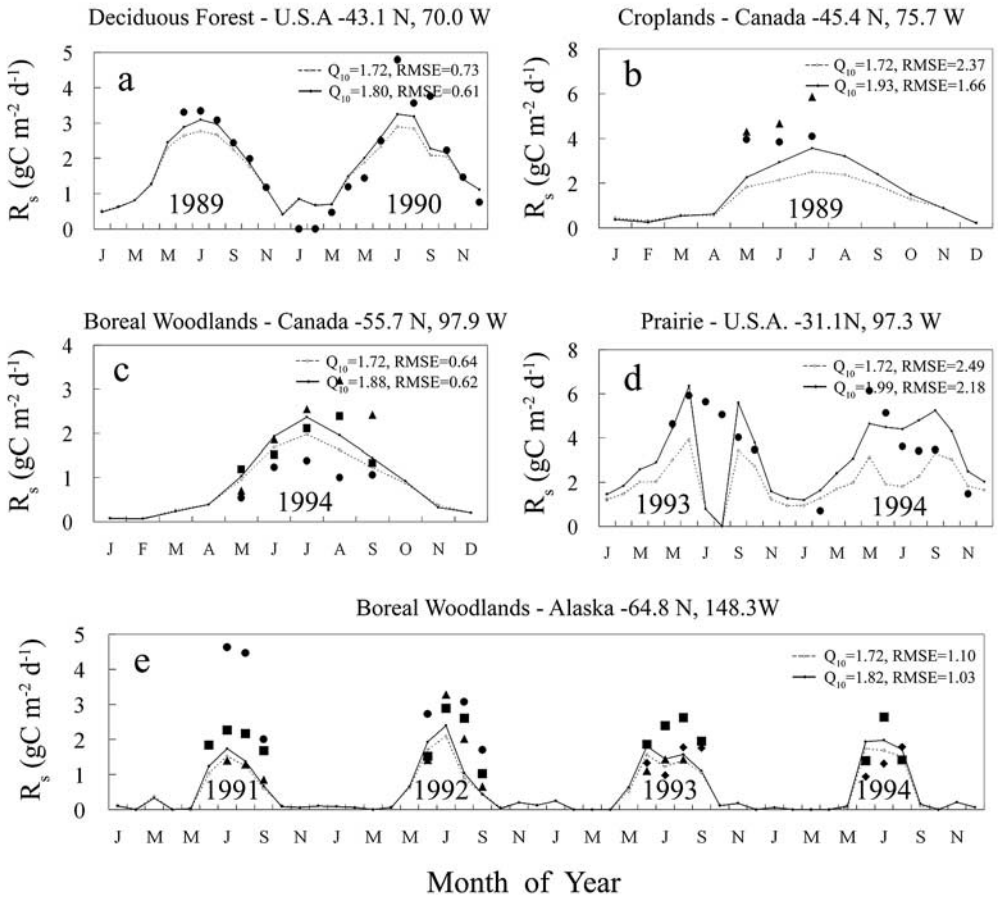

Figure 3. Comparisons between measured (solid symbols) and estimated soil respirations in various ecosystems. Dashed line is the values estimated by Raich's globally invariant Q_{10} model (equation (7)), and solid line is the values fitted by modified Raich's model using the estimated site-specific Q_{10} values (equation (8)). RMSE is root-mean squared error. (a) Data from a mixed deciduous forest in New Hampshire, based on *Crill* [1991]. (b) Data from barley (solid circles) and fallow (solid triangles) fields in Ottawa, Canada, based on *Rochette et al.* [1992]. (c) Data from spruce (solid circles), aspen (solid triangles), and pine (solid squares) woodlands in Manitoba, as estimated from Figure 3 of *Savage et al.* [1997]. (d) Data from a tallgrass prairie in Texas, as estimated from Figure 3 of *Mielnick and Dugas* [2000]. (e) Data from taiga forest stands in interior Alaska, as estimated from Figure 1 of *Gulledge and Schimel* [2000]: floodplain alder (solid circles); floodplain white spruce (solid triangles); upland birch and aspen (solid squares); and upland white spruce (solid diamonds).

[27] Under the second scenario with the actual observed interannual variation of temperature from 1982 to 1999, the temperature anomaly (i.e., the departure of the mean annual temperature from the total mean) ranged from −0.40 to 0.47. In correspondence, the anomaly of modeled soil respiration (i.e., the departure of modeled soil respiration in a particular year from the total mean during the period) ranges from −1.01 to 1.44 Pg C a^{-1} for the globally invariant Q_{10} value in model A and from −1.79 to 2.96 Pg C a^{-1} for spatially heterogeneous Q_{10} values in model B (Figure 5a). The linear regression between the anomaly of global mean annual temperature and the anomaly of modeled soil respiration has a slope of 1.88 Pg C $°C^{-1}$ for the globally invariant Q_{10} and 3.21 Pg C $°C^{-1}$ for the spatially heterogeneous Q_{10} values (Figure 5a). Although the temperature sensitivity of soil respiration estimated according to temperature anomaly under scenario 2 is less than that estimated under scenario 1 in the absolute magnitude, the relative magnitude of underestimation of the sensitivity by the globally invariant Q_{10} in comparison to that by the spatially heterogeneous Q_{10} is 41.4%, similar to that under scenario 1 (40.7%).

[28] Under scenario 2, soil heterotrophic respiration simulated by the CASA model has the temperature sensitivity of 2.26 Pg C $°C^{-1}$ when the spatially heterogeneous Q_{10} was considered (Figure 5b). As a comparison, the corresponding sensitivity is 1.69 Pg C $°C^{-1}$ (Figure 5b) with the globally invariant Q_{10}.

4. Discussion

4.1. Influences of Constraints on Estimation of Spatial Pattern of Q_{10}

[29] In this inverse analysis, we used spatially distributed measurements of soil organic carbon and several ancillary variables to constrain a process-based biogeochemical

Table 2. Correlations Between Q_{10} and Soil Organic Carbon and Nitrogen Content[a]

Land Cover Type	Q_{10} and SOC	Q_{10} and N
Broadleaf evergreen forest	0.56[b]	0.58[b]
Broadleaf deciduous forest and woodland	0.28[b]	0.32[b]
Mixed forest and woodland	0.39[b]	0.42[b]
Coniferous forest and woodland	0.67[b]	0.57[b]
High-latitude deciduous forest and woodland	0.84[b]	0.78[b]
Wooded C_4 grassland	0.48[b]	0.45[b]
C_4 grassland	0.38[b]	0.38[b]
Shrubs	0.11[b]	0.28[b]
Tundra	0.41[b]	0.34[b]
Desert, bare ground	0.23[b]	0.19[b]
Cultivation	0.22[b]	0.24[b]
C_3 wooded grassland	0.39[b]	0.42[b]
C_3 grassland	0.26[b]	0.28[b]
All vegetation	0.30[b]	0.31[b]

[a]SOC, soil organic carbon; N, nitrogen.
[b]Correlation is significant at the 0.01 level.

model so as to extract information on temperature sensitivity of soil heterotrophic respiration. We also used the global mean of the experimentally derived Q_{10} as a further constraint on estimation of the temperature sensitivity. Soil organic carbon originates from plant production and litter input. It accumulates slowly in soil to a steady state if there is no disturbance [*Li et al.*, 2004]. Therefore, the Q_{10} values derived from the observed soil organic carbon and relevant environmental factors are multiyear averaged temperature sensitivity, which is somewhat different from those derived from instantaneous measurements of soil respiration. The derived Q_{10} values from this inverse analysis are more suitable for projecting long-term climate-carbon cycle feedback at large spatial scales.

[30] Experimentally derived Q_{10} values from instantaneous soil respiration measurements reflect apparent temperature sensitivity at local scales and vary with many site-specific conditions [*Davidson and Janssens*, 2006]. The site-specific Q_{10} values cannot be easily scaled up to analysis at regional or global scales for at least two reasons. First, observations of soil respiration are too sparse and the ecosystems are too heterogeneous to allow large-scale assessment with sufficient accuracy [*Denman et al.*, 2007]. Second, experiment-based Q_{10} values are usually derived from regression analysis and can be unreasonably high or low due to confounding factors [*Davidson et al.*, 2006]. To avoid these issues, we used the global mean Q_{10} value as a constraint instead of the site-specific Q_{10} values.

[31] The inversion approach searched for optimal Q_{10} values by minimizing differences between modeled and observed SOC contents. The estimated Q_{10} values can be influenced by the inverse method, the model used in the analysis, and the searching range of Q_{10} values. When the experiment-based global mean Q_{10} value (= 1.72) was used as a constraint in the inverse analysis, the upper limit of Q_{max} equals 2.61 (Figure 1), which is amazedly similar to the value of 2.5 purely based on a theoretic analysis [*Davidson et al.*, 2006]. In addition, site-specific Q_{10} values

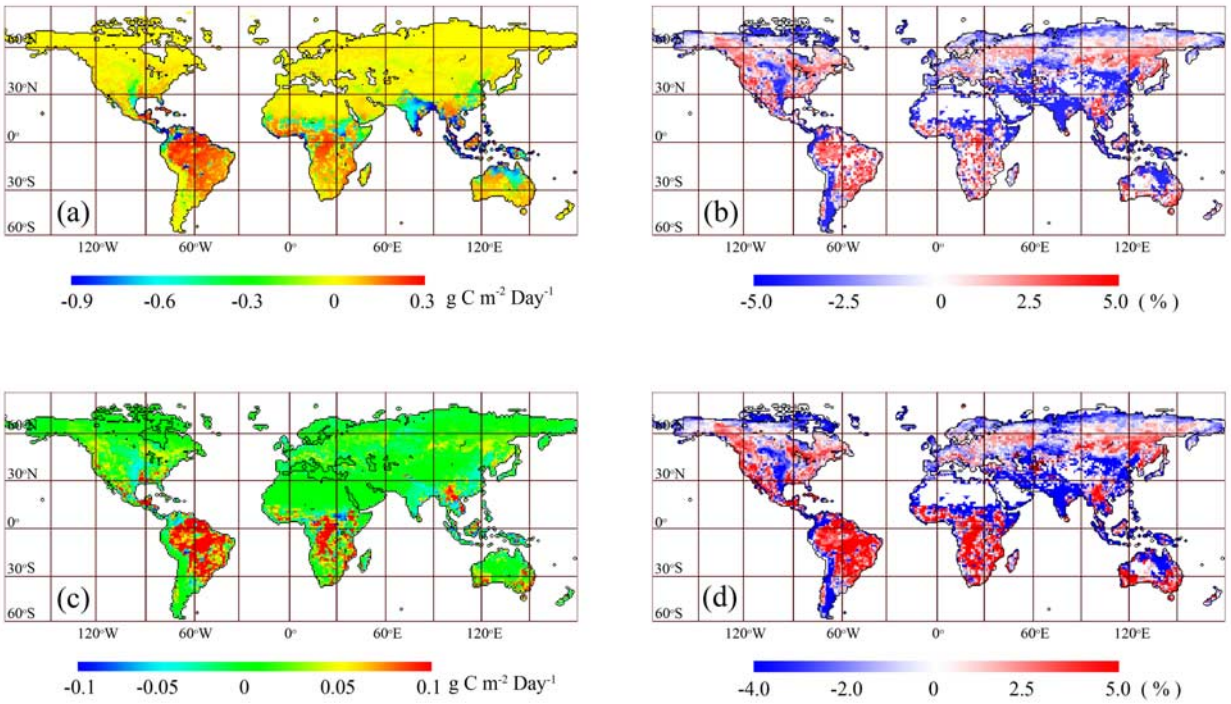

Figure 4. Absolute and relative discrepancies for total soil respiration and heterotrophic respiration increments modeled by the empirical and the process-based model at the scenario that temperature in each grid evenly increases 1°C. Absolute discrepancies for (a) total respiration and (c) heterotrophic respiration (modeled values of global invariant Q_{10} minus modeled value of spatial pattern of Q_{10}). Corresponding relative discrepancies for (b) total respiration and (d) heterotrophic respiration.

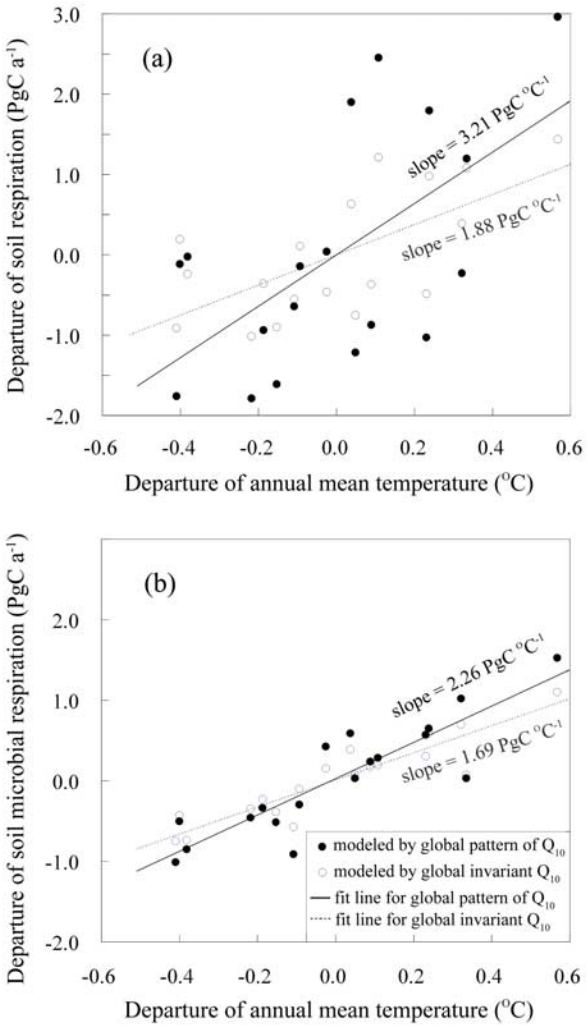

Figure 5. Relationship between the departure of annual soil respiration and annual mean temperature for 1982–1999. (a) Total soil respiration by empirical model and (b) soil heterotrophic respiration by process-based model.

derived from this inverse analysis provide better estimations of soil respiration with lower root-mean squared errors (RMSE) than the globally invariant Q_{10} (Figure 3). This further enhances the validity of the inversion method for estimation of Q_{10} values.

4.2. Spatially Variable Q_{10} Values and Their Impacts on Carbon Cycle–Climate Change Coupling

[32] One urgent mission in the Earth system science is to couple climate models with biosphere models to examine climate change–carbon cycle feedback [*Solomon et al.*, 2007]. However, the spatial resolution of climate system models is usually much larger than those of Q_{10} values derived form soil respiration measurements. As a consequence, newly derived Q_{10} values from ecological research could not be timely incorporated into the climate system models to improve our prediction of climate change. For example, it has been extensively illustrated by ecologists that Q_{10} values are spatially heterogeneous. The coupled models of a climate system with terrestrial carbon cycling, however, still use an assumed, globally invariant Q_{10} value [*Luo*, 2007]. The main cause is that ecosystems are too heterogeneous to allow a global assessment with sufficient accuracy [*Denman et al.*, 2007]. In this study we retrieved a spatial pattern of heterogeneous Q_{10} values at the 1° by 1° resolution based upon two considerations. First, the global data sets at 1° by 1° are plenteous for inversion algorithm. Second, this spatial resolution is matched with the general atmospheric circulation models (GCMs) and therefore useful for research on the climate-carbon feedback.

[33] The feedback intensity of global warming and soil carbon release depends not only on the magnitude of a global mean Q_{10} value but also their spatial variability. Our analysis on interannual variability in soil respiration caused by temperature anomaly indicates that the feedback intensity of total soil respiration and heterotrophic respiration to climate warming is 1.88 Pg C $°C^{-1}$ and 1.69 Pg C $°C^{-1}$, respectively, when a global invariant Q_{10} value was used. When spatially heterogeneous Q_{10} values were incorporated into models, the feedback intensity of total soil respiration and heterotrophic respiration is 3.21 Pg C $°C^{-1}$ and 2.26 Pg C $°C^{-1}$, respectively. Thus, a coupled climate-carbon cycle model that ignores spatial heterogeneity of Q_{10} would underestimate soil respiration by approximately 40% and heterotrophic respiration by about 25%.

5. Conclusions

[34] Temperature sensitivity of soil respiration (as indicated by Q_{10}) and its spatial variability are crucial for projecting climate change and atmospheric CO_2 concentration in the future. Our inverse analysis show that the observed soil organic carbon content and soil respiration offer good constraints on estimation of Q_{10} values in different spatial grids. Estimated Q_{10} values have a high spatial heterogeneity and are regulated by many spatially heterogeneous environmental factors. Q_{10} values vary with biome types and, in general, are higher at high-latitudinal bands. The derived spatially heterogeneous Q_{10} values result in better soil respiration estimation at different sites than the globally invariant Q_{10}. The feedback intensity of total soil respiration and heterotrophic respiration to climate warming would be underestimated by about 40% and 25%, respectively, if a globally invariant Q_{10} rather than spatially heterogeneous Q_{10} values are used in models.

[35] **Acknowledgments.** We thank Chris Field for sharing the source codes of CASA model and two anonymous referees for their valuable comments. We also thank the IGBP-DIS for providing the global carbon and nitrogen data set, Cort J. Willmott and Kenji Matsuura for providing the global climate data sets, Distributed Active Center at Goddard Space Flight Center, sponsored by NASA's Mission to Planet Earth program, for providing global 1° × 1° spatial resolution data sets of NDVI, solar radiation, soil type and texture, and land cover type. This study was supported by the National Natural Science Foundation of China (40671173, 40425008, 30590384, and 40401028), the Free Research Foundation of State Key Laboratory of Earth Surface Processes and Resource Ecology (070105), and the Terrestrial Carbon Program at the Office of Science, U.S. Department of Energy (DE-FG03-99ER62800).

References

Boone, R. D., K. J. Nadelhoffer, J. D. Canary, and J. P. Kaye (1998), Roots exert a strong influence on the temperature sensitivity of soil respiration, *Nature*, *396*, 570–572.

Cox, P. M., R. A. Betts, C. D. Jones, S. A. Spall, and I. J. Totterdell (2000), Acceleration of global warming due to carbon-cycle feedbacks in a coupled climate model, *Nature*, *408*, 184–187.

Crill, P. M. (1991), Seasonal patterns of methane uptake and carbon dioxide release by a temperate woodland soil, *Global Biogeochem. Cycles*, *5*, 319–334.

Davidson, E. A., and I. A. Janssens (2006), Temperature sensitivity of soil carbon decomposition and feedbacks to climate change, *Nature*, *440*, 165–173.

Davidson, E. A., E. Belk, and R. D. Boone (1998), Soil water content and temperature as independent or confound factors controlling soil respiration in a temperate mixed hardwood forest, *Global Change Biol.*, *4*, 217–227.

Davidson, E. A., I. A. Janssens, and Y. Luo (2006), On the variability of respiration in terrestrial ecosystems: Moving beyond Q_{10}, *Global Change Biol.*, *12*, 154–164.

Denman, K. L., et al. (2007), Couplings between changes in the climate system and biogeochemistry, in *Climate Change 2007: The Physical Science Basis—The Fourth Assessment Report of the Intergovernmental Panel on Climate Change*, edited by S. Solomon et al., Cambridge Univ. Press, New York.

Fang, C., P. Smith, J. B. Moncrieff, and J. U. Smith (2005), Similar response of labile and resistant soil organic matter pools to changes in temperature, *Nature*, *433*, 57–59.

Field, C. B., J. T. Randerson, and C. M. Malmstrom (1995), Global net primary production: Combining ecology and remote sensing, *Remote Sens. Environ.*, *51*, 74–88.

Friedlingstein, P., G. Joel, C. B. Field, and I. Y. Fung (1999), Toward an allocation scheme for global terrestrial carbon models, *Global Change Biol.*, *5*, 755–770.

Friedlingstein, P., J. L. Dufresne, P. M. Cox, and P. Rayner (2003), How positive is the feedback between climate change and the carbon cycle?, *Tellus, Ser. B*, *55*, 692–700.

Friedlingstein, P., et al. (2006), Climate-carbon cycle feedback analysis: Results from the (CMIP)-M-4 model intercomparison, *J. Clim.*, *19*, 3337–3353.

Global Soil Data Task (2000), *Global Soil Data Products* [CD-ROM], Int. Geosphere-Biosphere Programme–Data and Inf. Serv., Distributed Active Arch. Cent., Oak Ridge Natl. Lab., Oak Ridge, Tenn.

Gulledge, J., and J. P. Schimel (2000), Controls on soil carbon dioxide and methane fluxes in a variety of Taiga forest stands in interior Alaska, *Ecosystems*, *3*, 269–282.

Holland, E. A., J. C. Neff, A. R. Townsend, and B. McKeown (2000), Uncertainties in the temperature sensitivity of decomposition in tropical and subtropical ecosystems: Implication for models, *Global Biogeochem. Cycles*, *14*, 1137–1151.

Hui, D., and Y. Luo (2004), Evaluation of soil CO_2 production and transport in Duke Forest using a process-based modeling approach, *Global Biogeochem. Cycles*, *18*, GB4029, doi:10.1029/2004GB002297.

Ise, T., and P. R. Moorcroft (2006), The global-scale temperature and moisture dependencies of soil organic carbon decomposition: An analysis using a mechanistic decomposition model, *Biogeochemistry*, *80*, 217–231.

Jones, C. D., P. Cox, and C. Huntingford (2003), Uncertainty in climate-carbon-cycle projections associated with the sensitivity of soil respiration to temperature, *Tellus, Ser. B*, *55*, 642–648.

Kirschbaum, M. U. F. (1995), The temperature dependence of soil organic matter decomposition, and the effect of global warming on soil organic C storage, *Soil Biol. Biochem.*, *27*, 753–760.

Legates, D. R., and C. J. Willmott (1990a), Mean seasonal and spatial variability global surface air temperature, *Theor. Appl. Climatol.*, *41*, 11–21.

Legates, D. R., and C. J. Willmott (1990b), Mean seasonal and spatial variability in gauge-corrected, global precipitation, *Int. J. Climatol.*, *10*, 111–127.

Li, T., Y. Zhao, and K. Zhang (2004), *Soil Geography*, Higher Educ. Press, Beijing.

Liski, J., H. Ilvesniemi, A. Mäkelä, and K. J. Westman (1999), CO_2 emissions from soil in response to climatic warming are overestimated-The decomposition of old soil organic matter is tolerant of temperature, *Ambio*, *28*, 171–174.

Lloyd, J., and J. A. Taylor (1994), On the temperature dependence of soil respiration, *Funct. Ecol.*, *8*, 315–323.

Luo, Y. (2007), Terrestrial carbon cycle feedback to climate warming, *Annu. Rev. Ecol. Evol. Syst.*, *38*, 683–712.

Luo, Y., and X. Zhou (2006), *Soil Respiration and the Environment*, Academic, San Diego, Calif.

Luo, Y., S. Wan, D. Hui, and L. L. Wallace (2001), Acclimatization of soil respiration to warming in a tall grass prairie, *Nature*, *413*, 622–625.

Mielnick, P. C., and W. A. Dugas (2000), Soil CO_2 flux in a tallgrass prairie, *Soil Biol. Biochem.*, *32*, 221–228.

Parton, W. J., D. S. Schimel, C. V. Cole, and D. S. Ojima (1987), Analysis of factors controlling soil organic matter levels in Great Plains grasslands, *Soil Sci. Soc. Am. J.*, *51*, 1173–1179.

Parton, W. J., A. R. Mosier, and D. S. Schimel (1988), Dynamics of C, N, P, and S in grassland soils, a model, *Biogeochemistry*, *5*, 109–131.

Potter, C. S., and S. A. Klooster (1997), Global model estimates of carbon and nitrogen storage in litter and soil pools: Response to changes in vegetation quality and biomass allocation, *Tellus, Ser. B*, *49*, 1–17.

Potter, C. S., et al. (1993), Terrestrial ecosystem production: A process model based on global satellite and surface data, *Global Biogeochem. Cycles*, *7*, 811–841.

Raich, J. W., and C. S. Potter (1995), Global patterns of carbon dioxide emissions from soils, *Global Biogeochem. Cycles*, *9*, 23–36.

Raich, J. W., and A. Tufekcioglu (2000), Vegetation and soil respiration: Correlations and controls, *Biogeochemistry*, *48*, 71–90.

Raich, J. W., C. S. Potter, and D. Bhagawati (2002), Interannual variability in global soil respiration, 1980–94, *Global Change Biol.*, *8*, 800–812.

Randerson, J. T., et al. (1996), Substrate limitations for heterotrophs: Implications for models that estimate the seasonal cycle of atmospheric CO_2, *Global Biogeochem. Cycles*, *10*, 585–602.

Raupach, M. R., et al. (2005), Model-data synthesis in terrestrial carbon observation: Methods, data requirements and data uncertainty specification, *Global Change Biol.*, *11*, 378–397.

Reichstein, M., et al. (2002), Ecosystem respiration in two Mediterranean evergreen Holm oak forests: Drought effects and decomposition dynamics, *Funct. Ecol.*, *16*, 27–39.

Reichstein, M., et al. (2003), Modeling temporal and large-scale spatial variability of soil respiration from soil water availability, temperature and vegetation productivity indices, *Global Biogeochem. Cycles*, *17*(4), 1104, doi:10.1029/2003GB002035.

Rochette, P., R. L. Desjardins, E. G. Gregorich, E. Pattey, and R. Lessard (1992), Soil respiration in barley (*Hordeum vulgare* L.) and fallow fields, *Can. J. Soil Sci.*, *72*, 591–603.

Savage, K., T. R. Moore, and P. M. Crill (1997), Methane and carbon dioxide exchanges between the atmosphere and northern boreal forest soils, *J. Geophys. Res.*, *102*, 29,279–29,288.

Schimel, D. S., et al. (1994), Climatic, edaphic, and biotic controls over storage and turnover of carbon in soils, *Global Biogeochem. Cycles*, *8*, 279–293.

Sollins, P., P. Homann, and B. A. Caldwell (1996), Stabilization and destabilization of soil organic matter: Mechanisms and controls, *Geoderma*, *74*, 65–105.

Solomon, S., D. Qin, M. Manning, Z. Chen, M. Marquis, K. B. Averyt, M. Tignor, and H. L. Miller (2007), *Contribution of Working Group I to the Fourth Assessment Report of the Intergovernmental Panel on Climate Change*, Cambridge Univ. Press, New York.

Taylor, B. R., D. Parkinson, and W. F. J. Parsons (1989), Nitrogen and lignin content as predictors of litter decay rates: A microcosm test, *Ecology*, *70*, 97–104.

Tedla, A., X. Zhou, B. Su, S. Wan, and Y. Luo (2009), Labile, recalcitrant, and microbial carbon and nitrogen pools of a tallgrass prairie soil in the U.S. Great Plains subjected to experimental warming and clipping, *Soil Biol. Biochem.*, *41*, 110–116.

Wan, S., and Y. Luo (2003), Substrate regulation of soil respiration in a tallgrass prairie: Results of a clipping and shading experiment, *Global Biogeochem. Cycles*, *17*(2), 1054, doi:10.1029/2002GB001971.

Xu, M., and Y. Qi (2001), Spatial and seasonal variations of Q_{10} determined by soil respiration measures at a Sierra Nevadan forest, *Global Biogeochem. Cycles*, *15*, 687–696.

Zhou, T., and Y. Luo (2008), Spatial patterns of ecosystem carbon residence time and NPP-driven carbon uptake in the conterminous United States, *Global Biogeochem. Cycles*, *22*, GB3032, doi:10.1029/2007GB002939.

D. Hui, Department of Biological Sciences, Tennessee State University, Nashville, TN 37209, USA.

Y. Luo, Department of Botany and Microbiology, University of Oklahoma, Norman, OK 73019, USA.

P. Shi and T. Zhou, State Key Laboratory of Earth Surface Processes and Resource Ecology, Beijing Normal University, Number 19, Xinjiekouwai Street, Beijing 100875, China. (tzhou@bnu.edu.cn)